Transformation of Yttrium-Doped Hydrated Zirconium into Tetragonal and Cubic Nanocrystalline Zirconia

X. Bokhimi,*,1 A. Morales,* A. García-Ruiz,† T. D. Xiao,‡ H. Chen,§ and P. R. Strutt§

Institute of Physics, The National University of Mexico (UNAM), A.P. 20-364, 01000 Mexico, Mexico; †UPIICSA, COFAA, The National Polytechnic Institute, Té No. 950 Esq. Resina, 08400 Mexico D.F., Mexico; ‡Inframat Corporation, 20 Washington Avenue, Suite 106, North Haven, Connecticut 06473; §Precision Manufacturing Center, PMC, University of Connecticut, Storrs, Connecticut 06269

Nanostructured yttrium-stabilized zirconia powders, with yttria concentrations between 0.0 and 10.0 mol%, were prepared via the hydrolysis of an aqueous solution of zirconyl and yttrium chloride, and ammonium hydroxide. Powder phases were characterized by using X-ray powder diffraction; their crystalline structures were refined with the Rietveld technique. When samples were annealed below 200°C, their diffraction patterns corresponded to an amorphous atom distribution and were independent of yttria concentration. The doped amorphous phases crystallized, at 400°C, into tetragonal or cubic nanocrystalline zirconia, which were stabilized by yttrium. These results suggest that yttrium atoms served as a substitute for zirconium atoms not only in the crystalline phases but also in the amorphous phases, which are determined by the fast condensation of zirconyl clusters. Nondoped samples contained a mixture of monoclinic and tetragonal nanocrystalline zirconia; those with 2.5 to 5.0 mol% yttria contained only the tetragonal zirconia nanophase, and those with 7.5 to 10.0 mol% had only the nanocrystalline cubic phase. The average crystallite size of the nanophases diminished when Y_2O_3 concentration was increased. © 1999 Academic Press

Key Words: **zirconyl cluster; nanocrystalline zirconia; yttrium-doped zirconia; tetragonal zirconia; cubic zirconia; hydrated zirconium; X-ray diffraction; Rietveld technique.**

1. INTRODUCTION

The amorphous structure of hydrated zirconium (a system with aquo, hydro, and oxo bindings) and its crystallization into nanophases of pure zirconia depend on the behavior of zirconyl cluster (Fig. 1), $(Zr_4(OH)_8(OH_2)_{16})^{8+}$ (1–3). The amorphous phase occurs because these clusters condense rapidly, avoiding crystallization, and has a local order similar to that of tetragonal zirconia.

Tetragonal and cubic zirconia can be stabilized by doping them with large cations like yttrium (4). Their synthesis

using solid-state reaction, with yttria and zirconia precursors, requires large atom diffusion, which involves high temperatures. When zirconia is synthesized using soft chemistry based on hydrolysis, the zirconyl cluster is always involved (1); therefore, when yttrium-doped zirconia is prepared by these methods, zirconyl cluster must be affected by yttrium atoms.

Hoping to obtain some information about the effect of yttrium on zirconyl cluster, we studied in detail the crystallography of nanocrystalline yttrium-doped zirconia (Y_2O_3/ZrO_2), prepared via an advanced chemical route. The evolution of the amorphous and crystalline phases and their average crystallite size was analyzed as a function of yttria concentration and temperature.

Due to its superior properties, considerable attention has been focused on the development of materials based on zirconia. For example, they are chemically stable, have high hardness and mechanics strength (5–7), exhibit refractoriness (8), and are good ionic conductors (9, 10).

Zirconia is widely used in thermal barrier coatings of advanced engines, where extremely high temperatures are required, as well as to prepare milling balls, refractors, oxygen sensors, fuel cells barriers, and electronic ceramics.

Pure microcrystalline zirconia can exist in three different crystalline phases. At low temperatures, the stable phase is monoclinic; it is transformed into a tetragonal phase when it is heated at 1170°C. This tetragonal structure is transformed into a cubic one when samples are heated at 2370°C. The above transformations are accompanied by a unit cell volume change that, in some cases, is used to improve the mechanical properties of this material (11).

The high-temperature crystalline phases can be stabilized at low temperatures. This occurs by doping zirconia with low-valent cations, such as Mg^{2+}, Ca^{2+}, Y^{3+}, and rare earth cations, which incorporate into zirconia crystalline structure, as substitutes for zirconium cations.

Many methods for the preparation of conventional micrometer and submicrometer-sized ZrO_2 have been
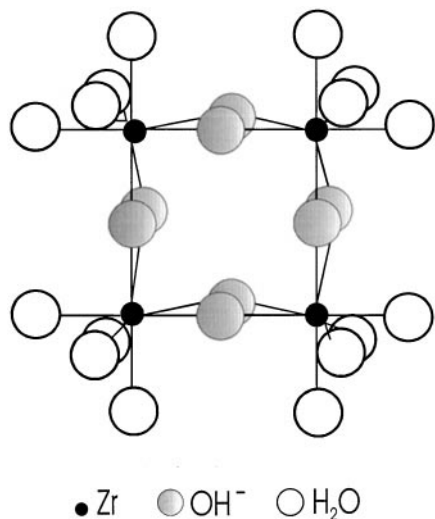

BOKHIMI ET AL.

FIG. 1. Tetrameric structural unit associated with the zirconyl cluster.

extensively developed (5–8, 12). These include coprecipitation, microemulsion, and sol-gel synthesis.

Recently, attention has been focused on reducing zirconia crystallite size from the micrometer to the nanometer dimensions; for example, spherical zirconia powders composed of crystallites with an average size of 20 nm were prepared by nebulized spray pyrolysis (13).

Nanostructured zirconia offers several advantages, especially at high temperatures (4, 14–16): low thermal conductivity, reduced sintering temperature, improved mechanical properties, and superplasticity. Currently, a number of production techniques are available for the synthesis of nanostructured oxide and nonoxide materials (17, 18). These include laser ablation, microwave plasma synthesis, spray conversion, flame pyrolysis, inert gas condensation, and sol-gel synthesis. These synthesis techniques are also being employed to prepare ultrafine and nanostructured Y_2O_3/ZrO_2 (4, 19–33).
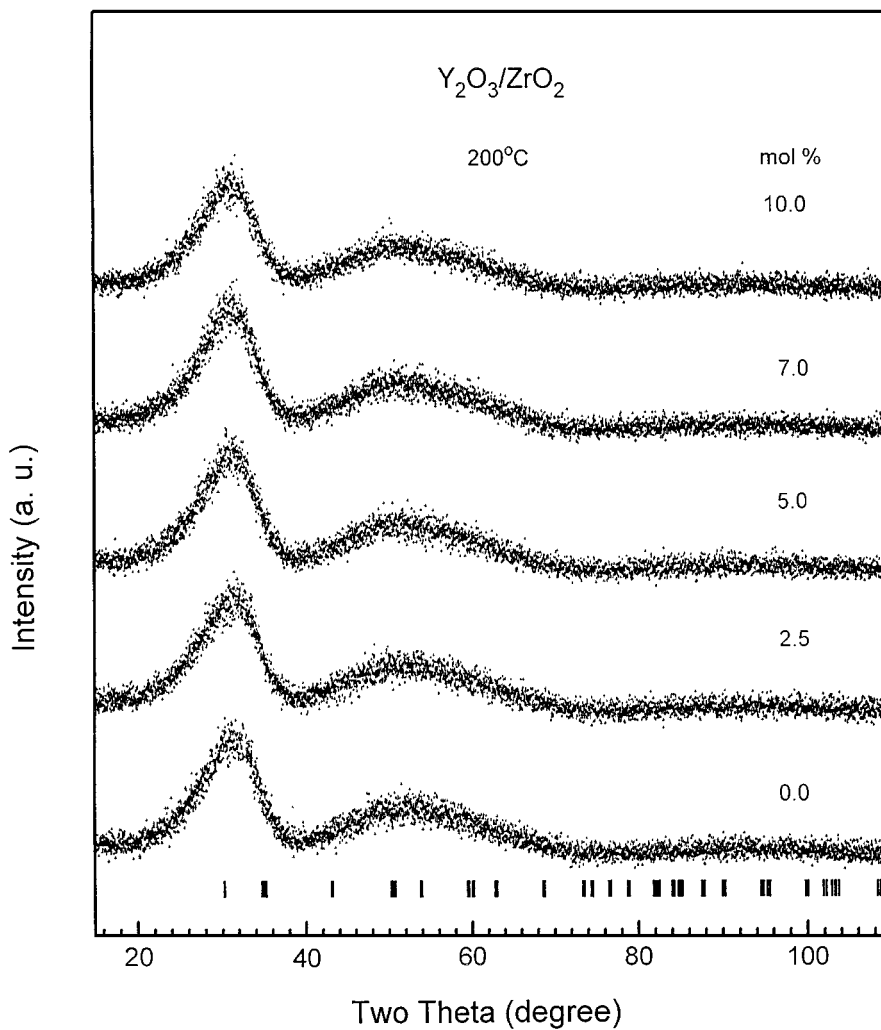

FIG. 2. X-ray diffraction patterns for the different yttria concentrations; samples were annealed in air at 200°C. Tick marks correspond to tetragonal zirconia.
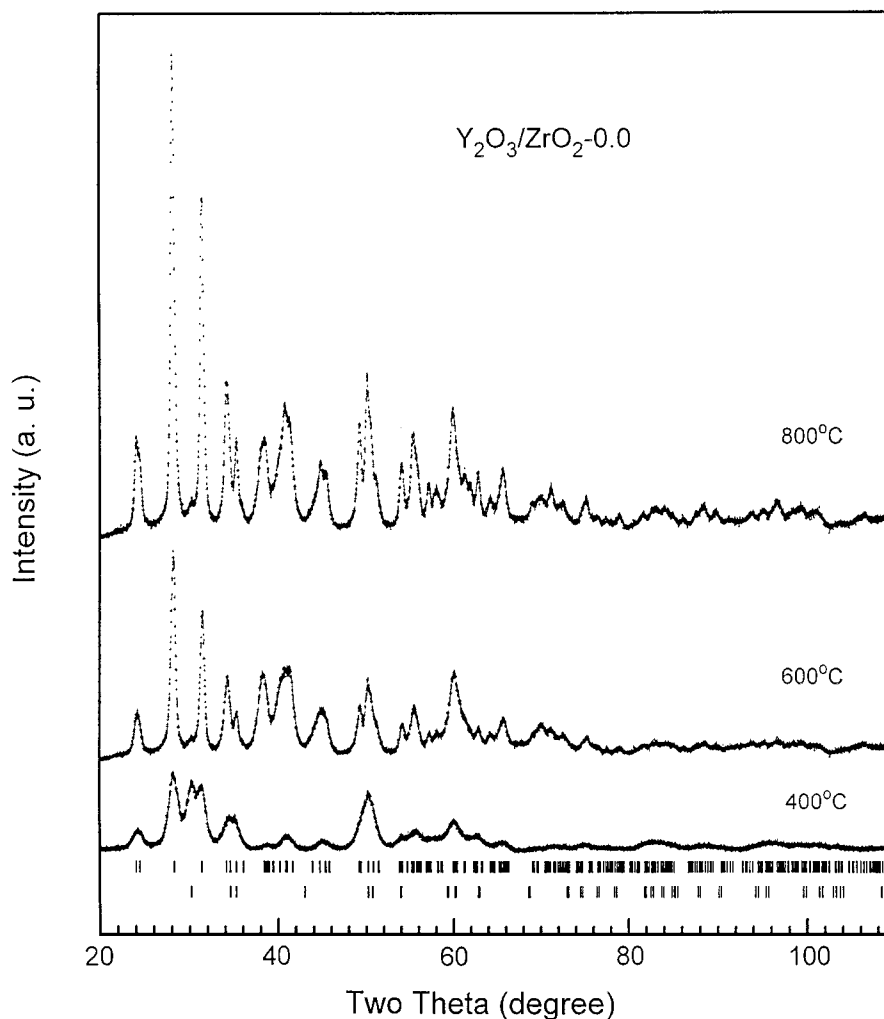
FIG. 3. X-ray diffraction patterns of nondoped samples annealed at different temperatures. Upper tick marks correspond to monoclinic zirconia; lower tick marks correspond to tetragonal zirconia.

In the present work, yttrium-doped zirconia was obtained via an advanced processing route that combines a precipitation hydrolysis with an atomized spraying and ultrasonic processing. Phase atomic arrangements (amorphous and crystalline) were analyzed in detail with X-ray powder diffraction, by refining the crystalline structures with the Rietveld technique.

2. EXPERIMENTAL

Sample Preparation

Y_2O_3/ZrO_2 powders were synthesized by hydrolysis. An aqueous solution of zirconyl chloride ($ZrOCl_2 \cdot 8H_2O$), yttrium chloride, and ammonium hydroxide (NH_4OH) was ultrasonically sprayed into the reaction vessel containing a diluted solution of NH_4OH in deionized water, while the vessel was vigorously stirred. The reaction product was ultrasonicated, dried, and then annealed at temperatures between 100 and 800°C to obtain nanostructured Y_2O_3/ZrO_2 powders. Yttria (Y_2O_3) concentrations were 0.0, 2.5, 5.0, 7.0, and 10.0 mol%.

Characterization

X-ray diffraction measurements were performed at room temperature with Cu$K\alpha$ radiation. Sample powders were packed in a glass holder. Intensity was measured by step scanning in the 2θ range between 20 and 110°, with a 2θ step of 0.02° for 2 s per point. Crystalline structures were refined with the Rietveld technique by using DBWS-9411 (34) and WYRIET (35) programs; peak profiles were modeled with a pseudo-Voigt (36) function that depends on average crystallite size (37). Standard deviations, which show the last figure variations of a number, are given in parentheses.
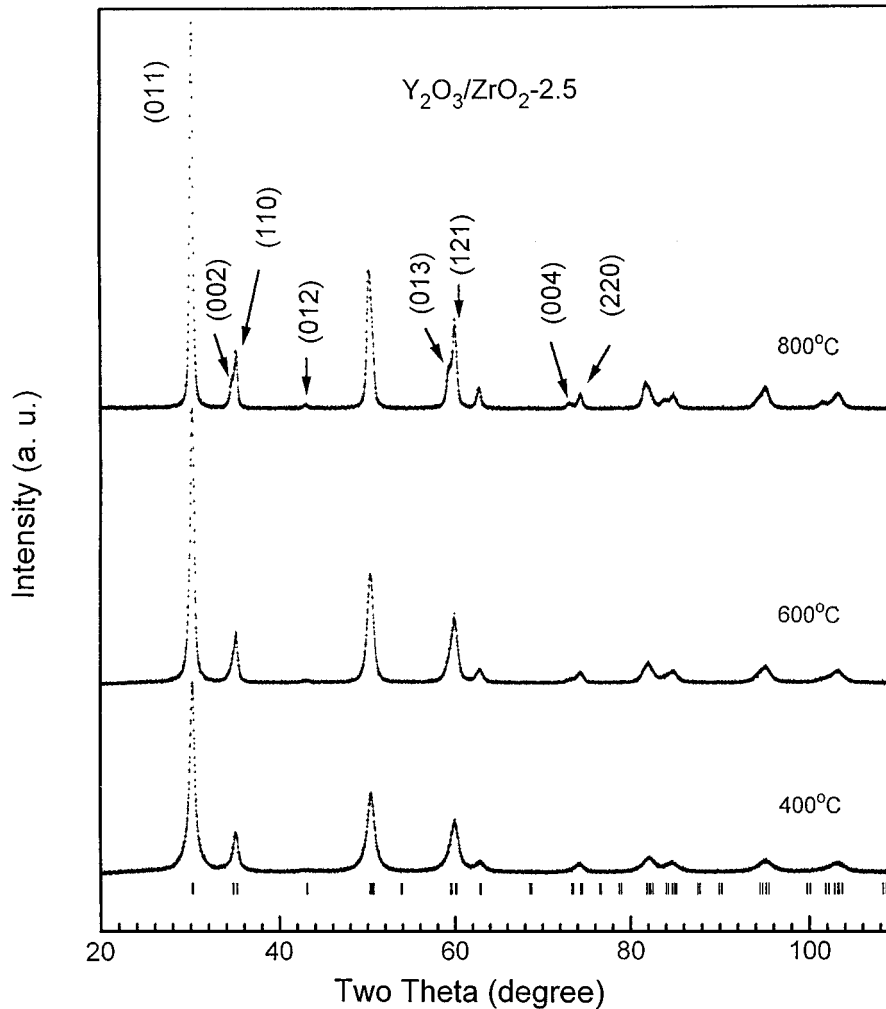
FIG. 4. X-ray diffraction patterns of the samples with 2.5 mol% yttria annealed at different temperatures. Tick marks and indices correspond to tetragonal zirconia.

When these deviations correspond to Rietveld refined parameters, their values are estimates not of the probable error in the analysis as a whole, but only of minimum possible probable errors based on their normal distribution (38).

3. RESULTS AND DISCUSSION

When the samples were annealed below 200°C, they were amorphous (Fig. 2) and crystallized when heated at 400°C (Figs. 3 through 7).

The X-ray diffraction patterns of the amorphous phases were equal and independent of yttrium concentration (Fig. 2). Despite the high yttrium concentrations, they had the same distribution observed in nondoped hydrated zirconium (3). This means that in some way, yttrium was dissolved into the hydrated-zirconium amorphous structure, forming an amorphous solid solution. As indicated by the

position of the main diffraction peak of the amorphous structure and the ticks corresponding to tetragonal zirconia (Fig. 2), the amorphous structure had the tetragonal zirconia local order.

The local order of the nondoped amorphous hydrated zirconium is determined by the zirconyl cluster $(Zr_4(OH)_8(OH_2)_{16})^{8+}$ (33, 39, 1). This cluster is a tetramer (Fig. 1) forming a lightly distorted square plane with four zirconium atoms at corners (40), similar to the faces of cubic zirconia (2, 41). A comparison of Clearfield's (40) and Bokhimi *et al.*'s (42) results on zirconia suggests that zirconyl symmetry is similar to the one observed in tetragonal zirconia, which is the phase formed when the amorphous phase crystallizes (42).

Since yttrium is dissolved in the amorphous phase, and this phase is based on zirconyl cluster, yttrium atoms could serve as a substitute for zirconium atoms in this cluster,
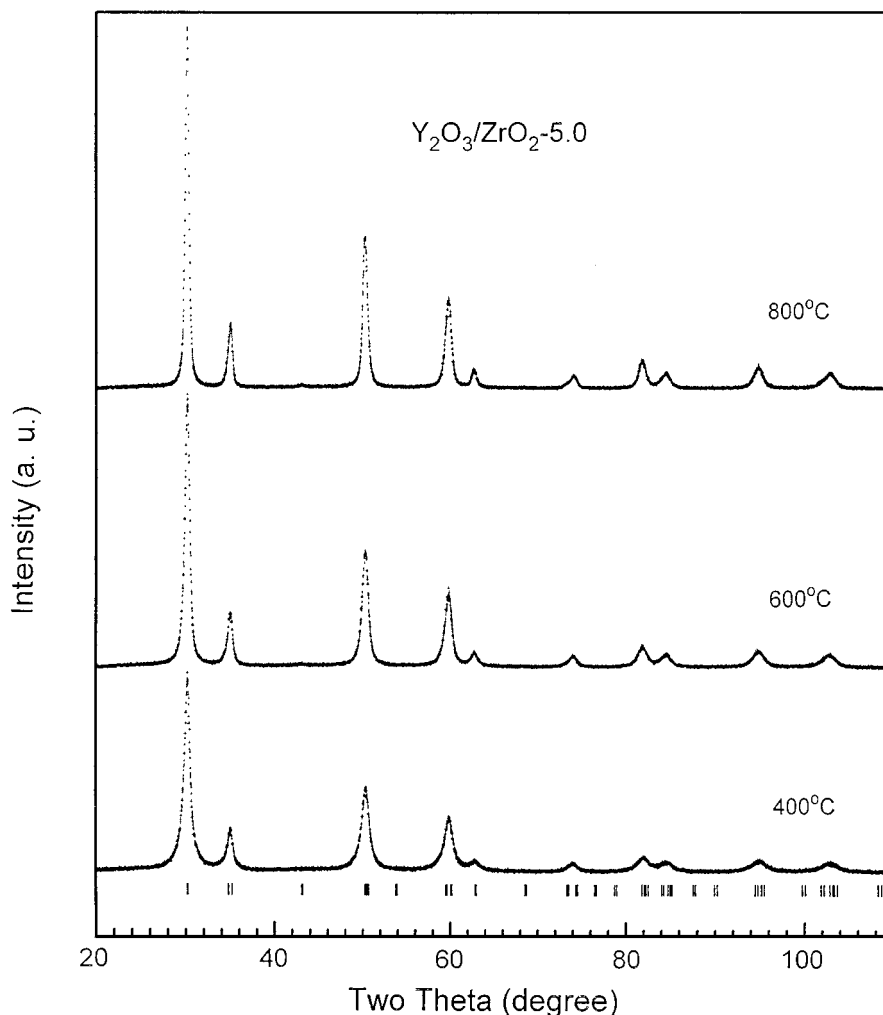
FIG. 5. X-ray diffraction patterns of the samples with 5.0 mol% yttria annealed at different temperatures. Tick marks correspond to tetragonal zirconia.

producing the yttrium-doped zirconyl ion $(Zr_{4(1-x)}Y_{4x}(OH)_8(OH_2)_{16})^{(8-4x)+}$. As in pure hydrated zirconium (1, 43), the yttrium-doped amorphous structure would occur by the fast condensation of these ions and zirconyl clusters via olation between tetramers. But, because yttrium valence is smaller than zirconium valence, some of the double hydroxyl bridges (Fig. 1) would have only one hydroxyl. The number of single-hydroxyl bridges will depend on yttrium concentration.

When samples were annealed at 400°C, the amorphous structure crystallized to nanocrystalline monoclinic, tetragonal or cubic zirconia, depending on yttria concentration. In the samples without yttrium, the crystallized phases were a mixture of monoclinic and tetragonal zirconia (Fig. 3). For 2.5 and 5.0 mol% Y_2O_3 only the tetragonal phase was observed (Figs. 4 and 5), but for 7.0 and 10.0 mol% Y_2O_3 the phase was cubic zirconia (Figs. 6 and 7).

To quantify the evolution of the crystalline phases with yttrium concentration and temperature, their crystalline structures were refined with the Rietveld technique. Cubic zirconia was refined with a cubic unit cell with space group $Fm3m$; tetragonal zirconia, with a tetragonal unit cell with space group $P4_2/nmc$; and monoclinic zirconia, with a monoclinic unit cell with space group $P2_1/c$. Figure 8 shows a typical Rietveld refinement plot.

Only the nondoped samples had monoclinic zirconia (Fig. 3). Its concentration, average crystallite size, and lattice parameters increased with temperature (Tables 1 and 2). In this system, stabilization of the tetragonal phase was produced by hydroxyl groups contained in its crystalline structure, as in sol-gel zirconia samples (42). The annealing above 400°C dehydroxylized the phase, destabilizing the tetragonal structure that eventually was transformed into monoclinic zirconia.
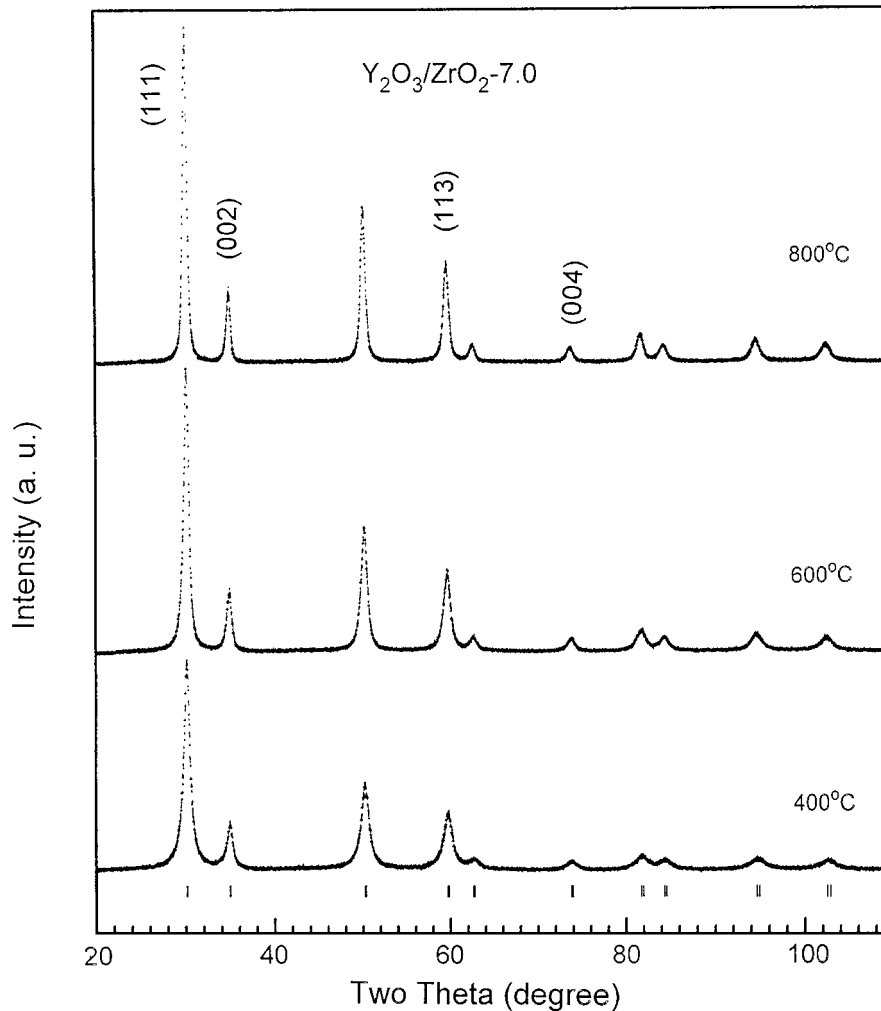
FIG. 6. X-ray diffraction patterns of the samples with 7.0 mol% yttria after they were annealed at different temperatures. Tick marks and indices correspond to cubic zirconia.

In yttrium-doped samples, the monoclinic phase was absent, even when they were annealed at high temperatures (Table 1). The absence of either monoclinic zirconia or segregated yttrium compounds indicated that yttrium was well dispersed in the samples. This result shows the goodness of the present synthesis method for preparing single-phase samples of nanocrystalline yttrium-doped zirconia.

As in microcrystalline samples, in the nanostructured zirconia reported in the present work yttrium stabilized its tetragonal and cubic phases (Table 1), but synthesis temperature was very low. In contrast to nondoped samples, the tetragonal phase was stable even when the sample was annealed at 800°C (Table 1).

Samples with 2.5 mol% Y_2O_3 had only nanocrystalline tetragonal zirconia (Fig. 4). Diffraction patterns of the samples annealed at 400 and 600°C had broad peaks that could

be associated to either a tetragonal or a cubic phase. They were modeled with a cubic and a tetragonal structure; the best fit corresponded to the tetragonal structure. The sample annealed at 400°C had a bimodal size distribution (Fig. 4 and Tables 1 and 3) that disappeared after annealing the sample at 600°C (Table 3).

The observable distinctive differences between cubic and tetragonal phases were the presence of the reflection (012) in the tetragonal phase (Fig. 4), and the splitting of the (002), (113), and (004) reflections of cubic phase (Fig. 6). Each of these three reflections split into two peaks of the tetragonal phase: (002), (110); (013), (121); and (004) (220) for (002), (113), and (004), respectively (Fig. 4). In the present case, the differences were more evident when the peak width decreased. For broad diffraction peaks, if one would assume a cubic phase, the split appeared as an apparent asymmetry of (002), (113), and (004) reflections (Fig. 6).
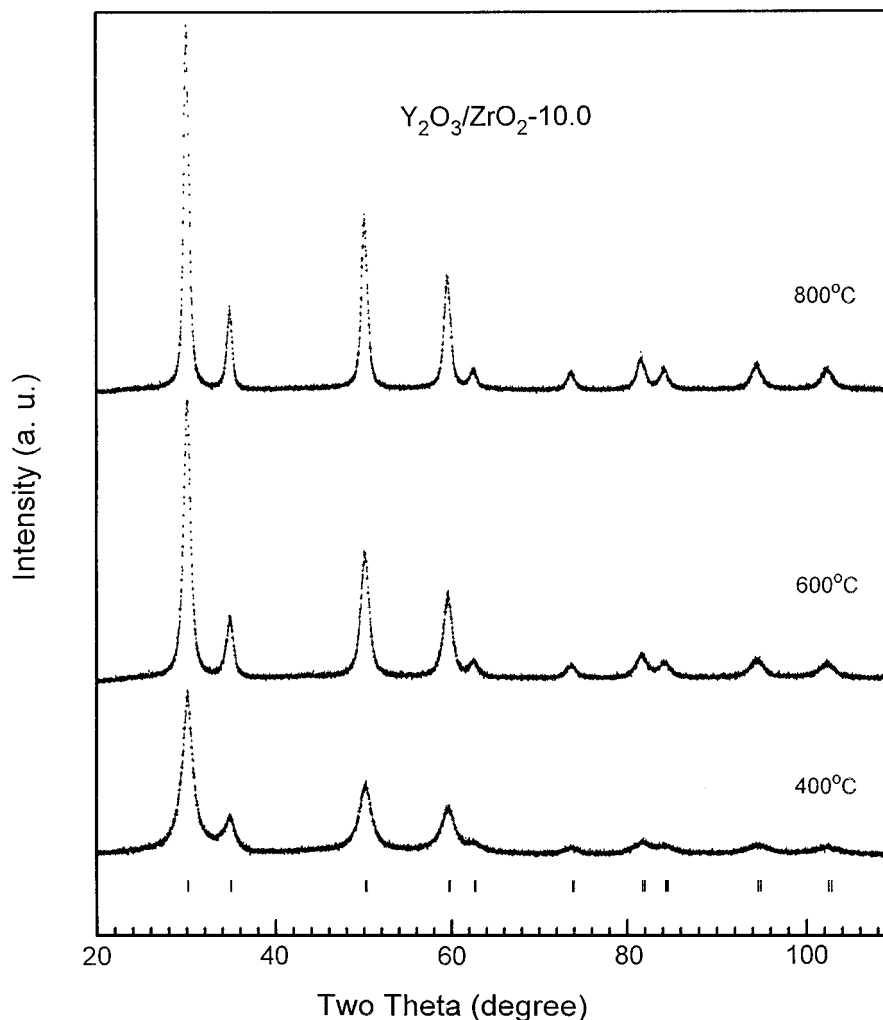
FIG. 7. X-ray diffraction patterns of the samples with 10.0 mol% yttria annealed at different temperatures. Tick marks correspond to cubic zirconia.

When Y_2O_3 concentration was 5.0 mol%, the structure was tetragonal, but the lattice parameters tended to correspond to a cubic phase; $c/(a\sqrt{2})$ ratio approached 1.0 (Table 3). The unit cell expanded slightly. In the diffraction patterns, the (002) and (110) reflections were not visually distinguished from each other, even when samples were annealed at 800°C; the refinement, however, distinguished them. For this yttria concentration, at a fixed annealing temperature, the average crystallite size was smaller than the one observed for 2.5 mol% yttria (Table 3).

For 7.0 mol% yttria, at all annealing temperatures, the sample had only nanocrystalline cubic zirconia (Fig. 6 and Table 1). The (002), (113), and (004) reflections did not show the asymmetry or splitting characteristic of the tetragonal structure. Lattice parameters slightly decreased with temperature (Table 4). At any annealing temperature, the average crystallite size was smaller than

one observed in the samples with 5.0 mol% Y_2O_3 (Tables 3 and 4).

The cubic structure was also the only one observed in the samples with 10.0 mol% Y_2O_3 (Fig. 7). The average crystallite size, however, was smaller than in the samples with 7.0 mol% yttria. It was 5.7 (2) nm when the sample was annealed at 400°C and increased to only 16.8 (3) nm after annealing the sample at 800°C. The increase on yttria concentration also expanded the unit cell (Table 4).

4. CONCLUSIONS

Via the synthesis method described in the present work, for yttria concentrations between 2.5 and 10 mol%, it was possible to produce single-phase tetragonal and cubic yttria-stabilized zirconia at temperatures as low as 400°C; the phases were nanocrystalline.
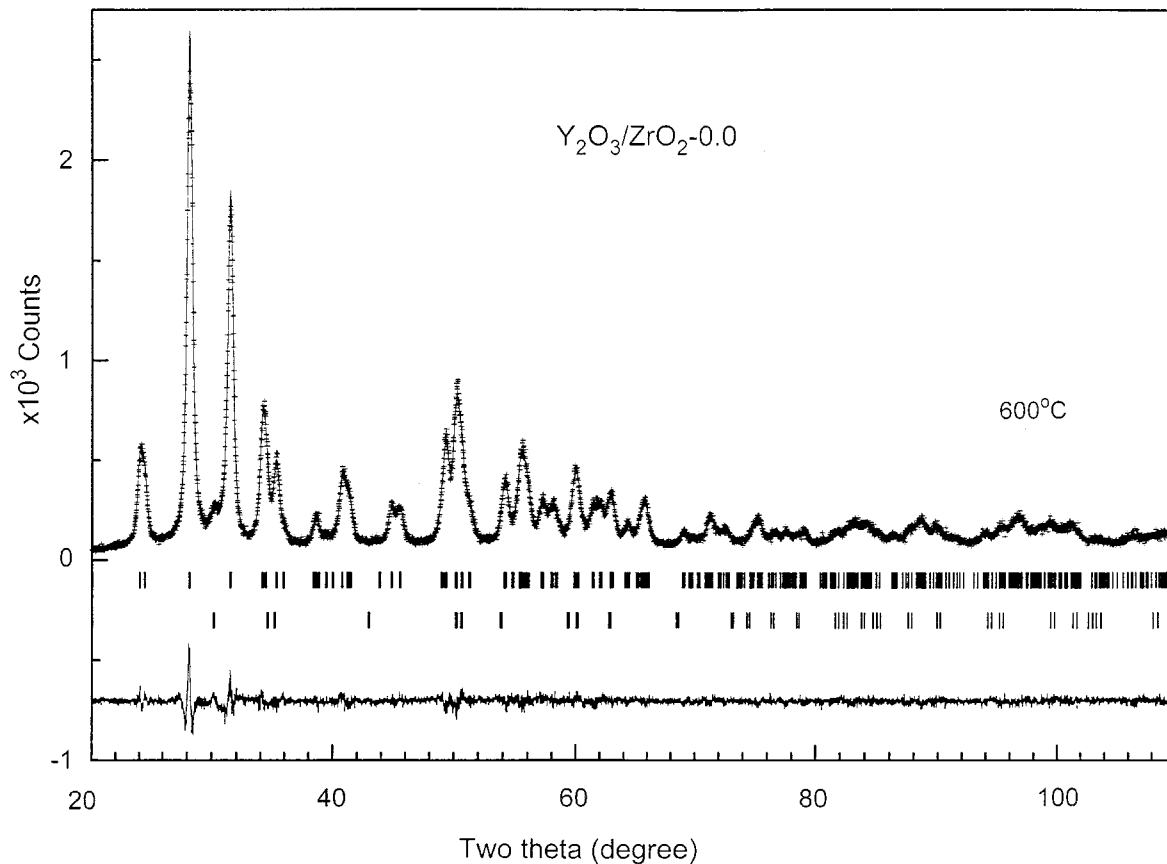
FIG. 8. Rietveld refinement plot of the non-doped sample after it was annealed at 600°C ($R_{wp} = 0.080$). Upper tick marks correspond to monoclinic zirconia ($R_F = 0.014$); lower tick marks correspond to tetragonal zirconia ($R_F = 0.012$).

TABLE 1
Zirconia: Phase Composition as a Function of Yttria Content and Temperature

Yttria concentration (mol%)	T (°C)	Cubic (wt%)	Tetragonal (wt%)	Monoclinic (wt%)
0.0	400	0.0	18.0 (1)	82.0 (1)
0.0	600	0.0	2.6 (1)	97.4 (1)
0.0	800	0.0	2.2 (1)	97.8 (1)
2.5	400	0.0	54.6 (5) 45.4 (4)	0.0
2.5	600	0.0	100.0	0.0
2.5	800	0.0	100.0	0.0
5.0	400	0.0	76 (1) 24 (1)	0.0
5.0	600	0.0	100.0	0.0
5.0	800	0.0	100.0	0.0
7.0	400	100.0	0.0	0.0
7.0	600	100.0	0.0	0.0
7.0	800	100.0	0.0	0.0
10.0	400	100.0	0.0	0.0
10.0	600	100.0	0.0	0.0
10.0	800	100.0	0.0	0.0

Yttrium-doped samples annealed at 200°C were amorphous. Their X-ray diffraction patterns were independent of yttrium concentration and identical to the one observed in the nondoped samples. This result and the fact that the phases formed during crystallization contained yttrium in their crystalline structure suggest that yttrium atoms were incorporated in zirconyl molecular structure. The most likely structure sites for yttrium atoms in zirconyl cluster are those occupied by zirconium; this would transform this cluster into the yttrium-doped zirconyl ion, $(Zr_{4(1-x)}Y_{4x}(OH)_8(OH_2)_{16})^{(8-4x)+}$, which would be the basic ion of

TABLE 2
Monoclinic Zirconia: Lattice Parameters as a Function of Yttria Content and Temperature

Yttria concentration (mol %)	T (°C)	Average crystallite size (nm)	a (nm)	b (nm)	c (nm)	β (°)
0.0	400	12.3 (6)	0.5144 (2)	0.5183 (2)	0.5304 (2)	98.64 (2)
0.0	600	21.4 (6)	0.51448 (4)	0.52033 (4)	0.53131 (4)	99.20 (1)
0.0	800	30.4 (8)	0.51439 (2)	0.52030 (3)	0.53146 (3)	99.20 (1)

TABLE 3
Tetragonal Zirconia: Lattice Parameters as a Function of Yttria Content and Temperature

Yttria concentration (mol %)	T (°C)	Average crystallite size (nm)	a (nm)	c (nm)	$c/(a\sqrt{2})$
0.0	400	17 (2)	0.35952 (6)	0.5179 (2)	1.0196 (5)
0.0	600	18 (8)	0.3606 (2)	0.5179 (5)	1.0156 (9)
0.0	800	15 (10)	0.3600 (3)	0.518 (1)	1.0174 (2)
2.5	400	7.2 (6)	0.36089 (8)	0.5195 (2)	1.0186 (3)
		19.9 (5)	0.36064 (3)	0.51425 (7)	1.008 (5)
2.5	600	20.8 (4)	0.3606 (2)	0.5160 (4)	1.0120 (6)
2.5	800	37.1 (6)	0.3605 (1)	0.5168 (2)	1.0137 (4)
5.0	400	6 (1)	0.3649 (3)	0.5207 (7)	1.009 (1)
		12 (2)	0.36126 (3)	0.5146 (1)	1.007 (2)
5.0	600	16.5 (3)	0.36177 (4)	0.51146 (1)	0.9997 (1)
5.0	800	26.2 (4)	0.36155(1)	0.51560 (4)	1.0084 (1)

yttrium-doped amorphous structures. This novel idea, however, must be confirmed by analyzing the samples with other techniques more sensitive to the atomic local order of amorphous atomic distributions.

When samples were annealed at 400°C, they crystallized into nanocrystalline zirconia with cubic, tetragonal, or monoclinic symmetry, depending on yttria concentration. Crystal symmetry increased with yttrium concentration.

The average crystallite size diminished as the yttrium concentration increased. This was probably due to an increase of the microstrains in the crystals caused by the difference in size and valence between zirconium and yttrium cations. Because of this, the samples with high yttrium concentration must be very rough and could have interesting catalytic properties.

TABLE 4
Cubic Zirconia: Lattice Parameters as a Function of Yttria Content and Temperature

Yttria concentration (mol%)	T (°C)	Average crystallite size (nm)	(nm) a
7.0	400	8.7 (5)	0.51334 (4)
7.0	600	14.6 (3)	0.51327 (2)
7.0	800	22.4 (4)	0.51320 (2)
10.0	400	5.7 (2)	0.51415 (7)
10.0	600	11.4 (2)	0.51388 (3)
10.0	800	16.8 (3)	0.51371 (2)

REFERENCES

1. A. Clearfied, *J. Mater. Res.* **5,** 161 (1990).
2. A. Clearfield, *Inorg. Chem.* **3,** 146 (1964).
3. G. T. Mamott, P. Barnes, S. E. Tarling, S. L. Jones, and C. J. Norman, *J. Mater Sci.* **26,** 4054 (1991).
4. S. Somiya, N. Yamamoto, and H. Yanagida, Eds., "Science and Technology of Zirconia III," *Advances in Ceramics*, Vols. 24A and 24B. American Ceramic Society, Westerville, OH, 1986.
5. N. Claussen, in "Science and Technology of Zirconia II" (N. Claussen, M. Ruhle, and A. H. Heuer, Eds.), American Ceramic Society, Columbus, OH, 1984.
6. R. C. Garvie, R. H. Hannink, and R. T. Pascoe, *Nature* **258,** 703 (1975).
7. A. G. Evans, D. B. Marshall, and N. H. Burlingame, in "Science and Technology," p. 202. Columbus, OH, 1981.
8. T. S. Busby, J. I. E. Conney, and J. Eccles, *Glass Technol.* **3,** 190 (1962).
9. A. M. Chirino and R. T. Sproule, *Am. Ceram. Soc. Bull.* **59,** 604 (1980).
10. S. P. S. Dadwal, *Solid State Ionic* **70/71,** 83 (1994).
11. Q.-M. Yuan, J.-Q. Tan, and Z.G. Jin, *J. Am. Ceram. Soc.* **69,** 265 (1986).
12. S. McRiani and C. Palmonaria, Eds., "Advances in Zirconia Science and Technology." Elsevier, New York/London, 1989.
13. P. Murugabel, M. Kalaiselvam, A. R. Raju, and C. N. R. Rao, *J. Mater. Chem.* **7,** 1433 (1997).
14. R. Birringer, H. Gleiter, H. P. Klein, and P. Marquardt, *Phys. Lett.* **102A,** 356 (1984).
15. H. Hahn and R. S. Averback, *J. Am. Ceram. Soc.* **74,** 2918 (1991).
16. G. Skandan, H. Hahn, B. H. Kear, M. Roddy, and W. R. Cannon, *Mat. Res. Soc. Symp. Proc.* **351,** 207 (1994).
17. R. Biringer, H. Gleiter, and R. W. Calm, Eds., "Encyclopedia of Materials Science and Engineering Suppl.," Vol. 1, Pergamon, Oxford, 1988.
18. M. Benaissa, M. José-Yacamán, J. M. Hernández, Bokhimi, K. E. Gonsalves, and G. Carlson, *Phys. Rev. B* **54,** 17763 (1996).
19. J. L. Shi, Z. X. Lin, W. J. Qian, and T. S. Yen, *J. Europe Ceram. Soc.* **13,** 265 (1994).
20. M. P. Otoole and R. J. Card, *Ceram. Bull.* **66,** 1486 (1987).
21. A. W. L. Dudeney, M. Abdel Ghani, G. I. I. Kelshall, A. J. Monhemius, and L. Zhang, *Powder Tech.* **65,** 207 (1991).
22. S. L. Dole, R. W. Scheldecker, L. E. Shiers, M. F. Berard, and O. Hunter, Jr., *Mater. Sci. Eng.* **32,** 277 (1978).
23. J. G. Duh, H. T. Dai, and W. Y. Hsn, *J. Mat. Sci.* **23,** 2786 (1988).
24. D. Burgard, C. Kropf, R. Nass, and H. Schmidt, *Mat. Res. Soc. Symp. Proc.* **346,** 101 (1994).
25. B. Duricie, D. Kolar, and M. Kornac, *J. Mater. Sci.* **25,** 1132 (1990).
26. S. C. Zhang and G. L. Messing, *J. Am. Ceram. Soc.* **73,** 61 (1990).
27. B. Fegley, Jr., P. White, and H. K. Bowen, *Ceram. Bull.* **64,** 1115 (1985).
28. M. L. Yanovskaya, N. M. Kotova, L. E. Obvinstseva, E. P. Turevskaya, N. Y. A. Turova, K. A. Vorotilov, L. I. Solovyova, and E. P. Kovsman, *Mater. Res. Soc. Symp. Proc.* **346,** 15 (1994).
29. R. Guinebretiere, A. Dauger, A. Lecomte, and H. Vestegehm, *J. Non-Cryst. Solids* **147/148,** 542 (1992).
30. L. L. Ilench and D. R. Ulrich, "Sciences of Chemical Processing." Wiley, New York, 1986.
31. D. Vollath and D. V. Szabo, *Nanostruct. Mater.* **4,** 927 (1994).
32. C. R. Aita, *Nanostruct. Mater.* **4,** 257 (1994).
33. J. G. Darab, M. F. Uehler, J. C. Linehan, and D. W. Matson, *Mater. Res. Soc. Symp. Proc.* **346,** 499 (1994).
34. R. A. Young, A. Sakthivel, T. S. Moss, and C. O. Paiva-Santos, *J. Appl. Crystallogr.* **28,** 366 (1995).

35. Margarita Schneider EDV - Vertrieb Starnbergweg 18, D-8134 Pöcking Germany, 1992.

36. P. Thompson, D. E. Cox, and J. B. Hasting, *J. Appl. Crystallogr.* **20,** 79 (1987).

37. R. A. Young and P. Desai, *Arch. Nauki Mat*. **10,** 71 (1989).

38. E. Prince, *J. Appl. Crystallogr*. **14,** 157 (1981).

39. G. M. Muha and P. A. Vaughan, *J. Chem. Phys*. **33,** 194 (1960).

40. A. Clearfield and P. A. Vaughan, *Acta Crystallogr.* **9,** 555 (1956).

41. G. Lundgren, *Svensk. Kem. Tidskr*. **71,** 200 (1959).

42. X. Bokhimi, A. Morales, O. Novaro, M. Portilla, T. López, F. Tzompanzi, and R. Gómez, *J. Solid State Chem*. **135,** 28 (1998).

43. X. Turrillas, P. Barnes, S. E. Tárling, S. L. Jones, C. J. Norman, and C. Ritter, *J. Mater. Sci. Lett*. **12,** 223 (1993).